ELSEVIER

Biophysical Chemistry 129 (2007) 70–81

Biophysical Chemistry

http://www.elsevier.com/locate/biophyschem

A model for triple helix formation on human telomerase reverse transcriptase (hTERT) promoter and stabilization by specific interactions with the water soluble perylene derivative, DAPER

Luigi Rossetti [a], Giuliana D'Isa [b], Clementina Mauriello [a], Michela Varra [b], Pasquale De Santis [c], Luciano Mayol [b], Maria Savino [a,d,*]

[a] *Dipartimento di Genetica e Biologia Molecolare, Università di Roma "La Sapienza", Piazzale Aldo Moro, 5, c.a.p. 00185, Roma, Italy*
[b] *Dipartimento di Chimica delle Sostanze Naturali, Università di Napoli Federico II, via D. Montesano 49, I-80131 Napoli, Italy*
[c] *Dipartimento di Chimica, Università di Roma "La Sapienza", Piazzale Aldo Moro, 5, c.a.p. 00185, Roma, Italy*
[d] *Istituto di Biologia e Patologia Molecolare del CNR, Università di Roma "La Sapienza", Piazzale Aldo Moro, 5, c.a.p. 00185, Roma, Italy*

Received 20 March 2007; received in revised form 14 May 2007; accepted 14 May 2007
Available online 21 May 2007

Abstract

The promoter of human telomerase reverse transcriptase (hTERT) gene, in the region from −1000 to +1, contains two homopurine–homopyrimidine sequences (−835/−814 and −108/−90), that can be considered as potential targets to triple helix forming oligonucleotides (TFOs) for applying antigene strategy.

We have chosen the sequence (−108/−90) on the basis of its unfavorable chromatin organization, evaluated by theoretical nucleosome positioning and nuclease hypersensitive sites mapping. On this sequence, anti-parallel triplex with satisfactory thermodynamic stability is formed by two TFOs, having different lengths.

Triplex stability is significantly increased by specific interactions with the perylene derivative *N,N′*-bis[3,3′-(dimethylamino) propylamine]-3,4,9,10-perylenetetracarboxylic diimide (DAPER).

Since DAPER is a symmetric molecule, the induced Circular Dichroism (CD) spectra in the range 400–600 nm allows us to obtain information on drug binding to triplex and duplex DNA. The drug-induced ellipticity is significantly higher in the case of triplex with respect to duplex and, surprisingly, it increases at decreasing of DNA. A model is proposed where self-stacked DAPER binds to triplex or to duplex narrow grooves.

Keywords: DNA triple helix; Triplex forming oligonucleotide; Telomerase inhibition; hTERT promoter; Perylene derivative DAPER; Triplex and duplex–DAPER complexes

1. Introduction

Telomeres are specific DNA–protein complexes that provide a protective cap at the ends of linear eukaryotic chromosomes [1]. Telomeric DNA is characterized by short G-rich sequences (5–8 bp) repeated in tandem for a length which varies in different organisms. The 3′ ending strand is rich in guanines and extends in a single strand overhang, which is the substrate of telomerase, a ribonucleoprotein reverse transcriptase enzyme, involved in the maintenance of telomere length [2,3].

Telomerase is active in almost all human tumors in addition to germinal and stem cells, but not in somatic cells [4]. In the last few years, there have been considerable efforts in producing telomerase inhibitors as possible anti-cancer agents [5–7].

Many different approaches have been taken to inhibit telomerase expression and/or function using antisense oligonucleotides, ribozymes and modified nucleosides.

During the last 10 years there has been a development in the use of sequence specific oligonucleotides for regulating gene expression [8]. Both antisense [9] and antigene [10] strategies

* Corresponding author. Tel.: +39 06 49912238; fax: +39 06 4440812.
E-mail address: maria.savino@uniroma1.it (M. Savino).

0301-4622/$ - see front matter © 2007 Elsevier B.V. All rights reserved.
doi:10.1016/j.bpc.2007.05.009

have been used to inhibit the translation or the transcription process, respectively.

The antigene approach involves triple helix formation using oligonucleotides binding to homopurine–homopyrimidine sequences of duplex DNA. The triplex forming oligonucleotides (TFOs) binding occurs in the major groove, forming a specific complex stabilized by Hoogsteen or reverse Hoogsteen hydrogen bonds (Fig. 1a). As a result of destabilizing effect due to charge–charge repulsion [11], the association of a third strand with a duplex is a thermodynamically weaker and kinetically slower process than duplex formation. In some cases, specific ligands, that provide additional binding interactions, have been employed to enhance the stability of triple helix [12]; these ligands may bind to triple helix through different mechanisms such as intercalation and/or minor groove binding by hydrophobic as well as electrostatic interactions.

Homopurine–homopyrimidine tracts are frequently found in the upstream regulatory regions of genes and several TFOs have been shown to down-regulate expression of targeted genes by blocking transcription initiation [13–17].

In these premises, the possibility of influencing the transcription of hTERT gene, using TFOs directed to its promoter region, appears of great interest, although it has not been explored so far.

The hTERT promoter contains putative binding sites for several transcription factors, such as c-*myc* [18], SP1 [19], an Ets family protein (Ets2) [20] and estrogen receptors [21], thus suggesting complex regulation mechanisms [22]. Moreover, it has been recently shown that hTERT transcription was associated with the appearance of a major deoxyribonuclease I (DNase I) — hypersensitive site positioned nearby to the hTERT transcription start site [23], evidencing a dominant role

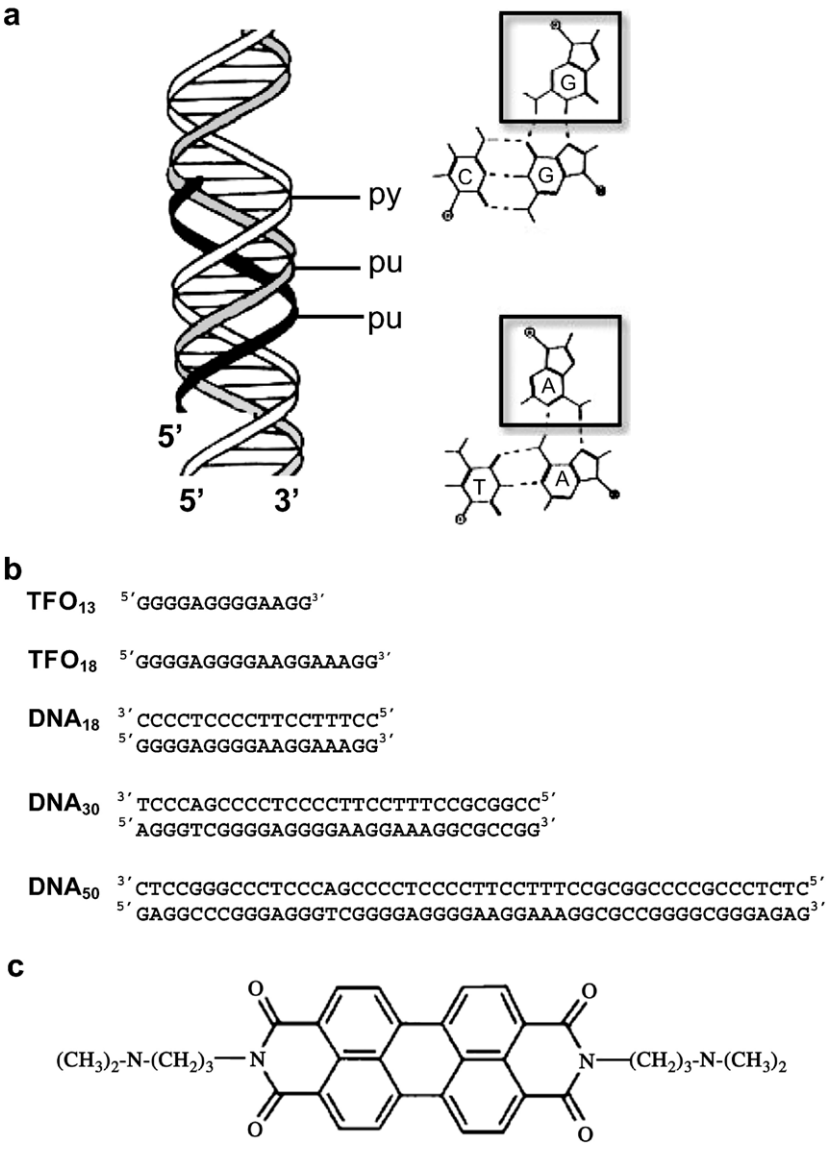

Fig. 1. (a) Pictorial drawing of the structure of anti-parallel triplex. (b) Triplex Forming Oligonucleotides (TFOs) and duplex DNAs sequences. (c) Structure of DAPER.

for the remodeling of this chromatin domain in the hTERT gene expression. Thus, this DNA tract should be accessible to regulative factors and to TFOs *in vivo*.

On the basis of its chromatin organization, evaluated by theoretical analysis of nucleosome positioning [24,25] and hypersensitive nuclease site mapping [23], we have identified the most accessible homopurine–homopyrimidine sequence of hTERT promoter and designed two TFOs directed to it. The sequence selected for triplex mediated gene target is located ~100 bp upstream transcription initiation site in hTERT gene.

We have synthesized two homopurine sequences having different lengths, which completely (TFO_{18}) or partially (TFO_{13}) overlap the homopurine–homopyrimidine target site (−108/−90 bp), both able to form triplex with satisfactory thermodynamic stability. Their thermodynamic stability is significantly increased by the interactions with the perylene derivative *N,N′*-bis[3,3′-(dimethylamino) propylamine]-3,4,9,10-perylenetetracarboxylic diimide (DAPER) [26], having positively charged side chains. It is worth noting that, at $MgCl_2$ physiological concentration (1 mM), triplex–DAPER complexes are stable, while triplex structures without DAPER, at the same experimental conditions, are unstable.

2. Experimental

2.1. Single stranded oligonucleotides

The single stranded oligonucleotides corresponding to DNA_{50} (Fig. 1b) were purchased from MWG-Biotech.

2.2. Oligonucleotides synthesis

The single stranded TFO_{13} and TFO_{18} and the two strands forming DNA_{30} and DNA_{18} (Fig. 1b) were synthesized on a 15 μmol scale *via* the phosphoramidite method, using a PERSEPTIVE Biosystems synthesizer, purified by ionic exchange High Performance Liquid Chromatography (HPLC) and successively desalted by molecular exclusion chromatography (Biogel P-2 fine). The purity was checked by reverse phase HPLC and electrophoresis in 20% denaturing polyacrylamide gel containing 7 M urea. Oligonucleotides were dissolved in water and the concentrations were determined spectrophotometrically by measuring absorbance at 260 nm and using extinction coefficients determined by a free oligonucleotide calculations program available on the sigma-aldrich site: http://proligo2.proligo.com/Calculation/calculation.html.

2.3. Theoretical modeling of nucleosome positioning

Few years ago, we have developed a theoretical method, based on sequence-dependent DNA curvature and flexibility, which allows the quantitative prediction of the free energy of nucleosome formation in terms of thermodynamics and structural parameters of the dinucleotide steps [24,25]. If $\Delta G(k)$ represents the nucleosome reconstitution free energy difference of the kth DNA tract (defined as the nucleosome with its dyad at kth position of the sequence) with $L=146$ bp along a sequence with N bp, the free energy *per* mole of nucleosome, ΔG, pertinent to the whole DNA is:

$$\beta\Delta G = -\ln \sum_{k=L/2}^{N-L/2} \exp[-\beta\Delta G(k)] \quad (1)$$

where β is $1/RT$. The exponential term represents the equilibrium constant pertinent to the nucleosome reconstitution of the kth DNA tract. The global reaction is considered as a sum of parallel reactions; for this reason the different equilibrium constants, pertinent to all the possible nucleosome positions, sum up.

Using a statistical thermodynamic approach we obtained $\Delta G(k)$ from the pertinent canonical partition functions. We evaluated the elastic contributions to the partition functions, related to the sum of the bending and twisting energies necessary to distort the intrinsic structure of the kth DNA tract in the nucleosomal form. Assuming first order elasticity we obtained [25]

$$\beta\Delta G_{el}(k) = \beta\Delta E^{\circ}_{el}(k) - 3/2(L \ln\langle T/T^{*}\rangle) + Z - Z\cos\varphi \quad (2)$$

where $\Delta E_{el}^{\circ}(k)$ is the minimum elastic energy required to distort the kth tract of L bp in the nucleosomal form; $\langle T/T^{*}\rangle$ is the average normalized dinucleotide empirical melting temperature of the kth DNA tract, which suitably represents the DNA differential rigidity; Z is equal to $(\beta b/L)\langle T/T^{*}\rangle A_n A_f$. $A_n A_f$ represents the correlation between the curvature of the nucleosomal DNA and that of the free form in terms of the Fourier transform amplitudes of frequency 0.17 of the nucleosome and the free DNA curvature function along the L bp tract of the sequence, according to the convolution theorem, and φ is the angle between the directions of the effective intrinsic curvature and the nucleosome dyad axis.

The theoretical free energy values so obtained, showed satisfactory agreement with the experimental data for a number of DNAs, but major deviations for others. This agreement, however, was strictly correlated ($R=0.99$) with the free DNA effective curvature, $\langle A_f\rangle$, which represents in modulus and phase the degree of similarity of the free DNA curvature with that of the nucleosome. This strongly indicated the existence of an additional curvature-dependent contribution to the free energy, which appears to destabilize the nucleosome. Such a contribution was obtained by fitting the free energy deviations by a quadratic function of the effective curvature [24,25]. We interpreted this free energy contribution as due to the groove contractions in intrinsically curved free DNAs, which stabilize the water spine and counterion interactions adding a further energy cost to the nucleosome formation. This contribution can be neglected for straight and slightly curved sequences.

If we calculate the free energy minima along a DNA sequence, long enough to accommodate more than one nucleosome, we can assume that the minima along the sequence represent virtual nucleosome positions.

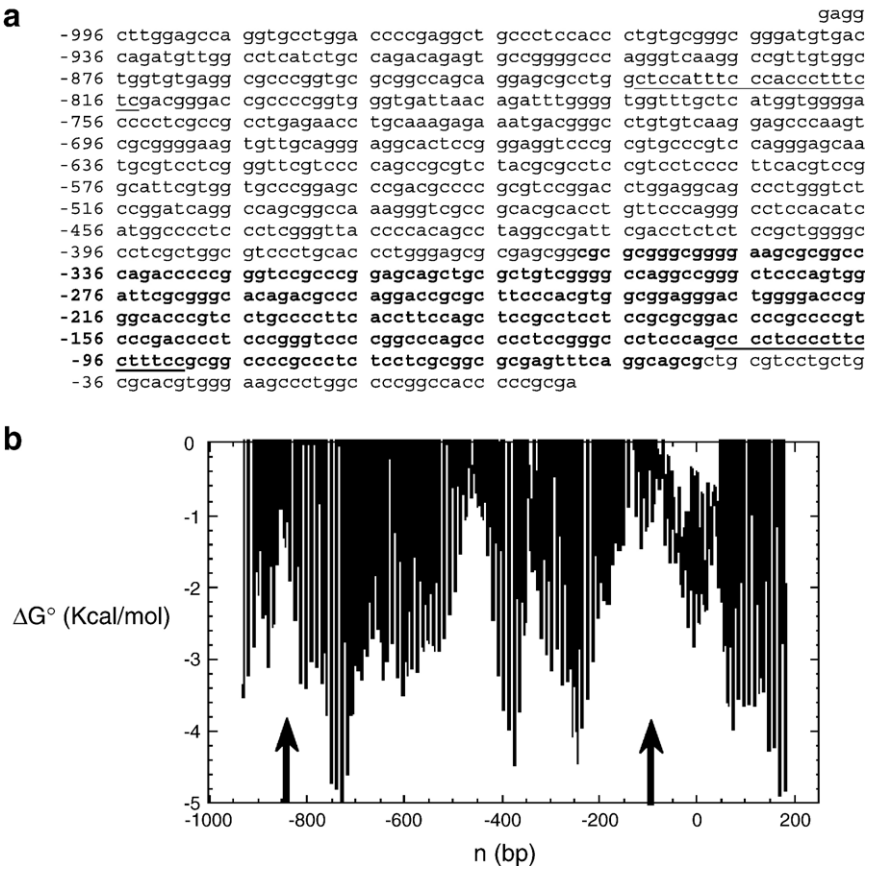

Fig. 2. (a) Sequence of the hTERT regulative region upstream to the transcription initiation site (−1000/+1). The homopurine–homopyrimidine tracts are underlined. Numbers to the left indicate bases upstream the ATG (position 1). Bold type sequence corresponds to hTERT F fragment. (b) Theoretical free energy difference of nucleosome formation with respect to the average nucleosome along the hTERT promoter. The arrows indicate the two homopurine–homopyrimidine tracts identified on the promoter and reported in (a).

2.4. Electrophoretic Mobility Shift Assays (EMSA)

EMSA were performed using as target a 50-mer duplex (DNA_{50}) corresponding to the hTERT promoter region from −124 to −74 containing the homopurine–homopyrimidine sequence located in the region −108/−90 (Fig. 1b).

The purine-rich strand was end labeled with [γ-^{32}P] ATP (3000 Ci/mmol Amersham Pharmacia Biotech) and T4 polynucleotide kinase (Fermentas); this strand was then annealed to the complementary pyrimidine strand, in slight excess (10 min at 95 °C and then allowing to slowly cool at 0 °C).

A fixed amount of labeled DNA_{50} (30 nM) was mixed with different amounts of TFOs (heated at 95 °C for 5 min to reduce self-aggregation) in standard buffer (STD buffer; 50 mM Tris–HCl pH 7.6, 50 mM NaCl and 5 mM $MgCl_2$) and incubated overnight at 37 °C. The samples were subsequently analyzed in a native 15% polyacrylamide gel (19:1 acrylamide:bisacrylamide ratio), run at 4 °C, for 18 h, at a constant voltage of 200 V, with recycling of the electrophoresis buffer (STD buffer).

The gels were scanned using the Instant Imager Packard and the amount of triplex formed was obtained quantifying the intensities of the duplex and triplex bands. The reaction that takes place in each sample is

$$DNA_{50} + TFO \rightleftarrows T \tag{3}$$

so that the association constant, K_a, is given by

$$K_a = [T]/[DNA_{50}]([TFO]_0 - [T]) \tag{4}$$

where $[T]$ and $[DNA_{50}]$ (labeled target) are equilibrium concentration of triplex and duplex target respectively, obtained by the quantitative evaluation of electrophoretic bands, and $[TFO]_0$ is the total concentration of TFO. Calculating the association constants, we considered $[TFO]_0 - [T] = [TFO]_0$, since the oligonucleotide is in large excess with respect to DNA_{50}.

The experiments in the presence of DAPER (Pierce), a water soluble perylene derivative (see Fig. 1c), reported in Fig. 5b, were carried out in the same experimental conditions, except than DAPER at suitable concentration, was added to the DNA mixtures, as last component. In this case, due to the significantly lower TFO concentration with respect to the experiments without DAPER, we have calculated the K_a values using the TFO actual concentrations as $[TFO]_0 - [T]$.

To evaluate the influence of K^+ ions with respect to Na^+ ions, in the presence of DAPER, the same procedure was adopted, except than KCl replaces NaCl. The EMSA, reported in Fig. 5c, were carried out lowering the $MgCl_2$ concentration from 5 mM to 1 mM.

2.5. UV spectroscopic temperature-dependent melting studies

UV thermal stability experiments were carried out with a JASCO 530 spectrophotometer equipped with ETC-505T temperature control. For triplex complexes, each sample contain 1:1 mixture of TFO_{13} or TFO_{18} and DNA_{30} of 35 μM of each oligonucleotide component, in 20 mM of Tris–HCl, pH 7.3, 50 mM NaCl and 5 mM $MgCl_2$. The samples were first annealed with the same procedure than for EMSA. Melting curves were obtained by monitoring the variation of absorbance at 260 nm with temperature from 10 to 90 °C. The heating rate was fixed at 0.5 °C/min.

2.6. Deoxyribonuclease I (DNase I) footprinting assay

A 260 bp fragment of hTERT promoter (−309/−50, hTERT F; Fig. 2a) containing the sequence −108/−90 was excised from the p1009 plasmid containing 1009 bp of hTERT promoter [27].

The plasmid was digested with Eco47 III and labeled at 5′ terminus with [γ-^{32}P]ATP by T4 polynucleotide kinase, so that the purine-rich strand is radioactively labeled. The plasmid was then digested with Pvu II. The resulting 260 bp fragment (hTERT F) was subsequently purified by preparative gel electrophoresis 5% polyacrylamide, 90 mM Tris Borate, 2 mM ethylene-diaminetetraacetic acid (EDTA) (TBE 1X). To obtain the same DNA fragment with pyrimidine-rich strand labeled, the order of restriction digestion was inverted. The fragment was then mixed with the TFO (13 mer or 18 mer) and the mixtures were incubated overnight at 37 °C in STD buffer. After incubation the samples were digested with (DNase I), 0.2 U, for 1 min at 37 °C, in STD buffer (50 mM Tris–HCl pH 7.6, 50 mM NaCl and 5 mM $MgCl_2$), and the reaction stopped by adding EDTA, pH 8 at 10 mM final concentration.

The samples were then immediately loaded on a 6% sequencing gel and electrophoresis carried out in TBE 1X, at 60 W for 2 h. Gels were dried and exposed to X-ray film; autoradiographies were analyzed by densitometric analysis.

The experiments, in the presence of DAPER, were carried out under the same experimental conditions.

2.7. Absorption and circular dichroism spectra

Absorption spectra were recorded on Jasco V530 spectrophotometer. Circular Dichroism (CD) spectra were recorded on

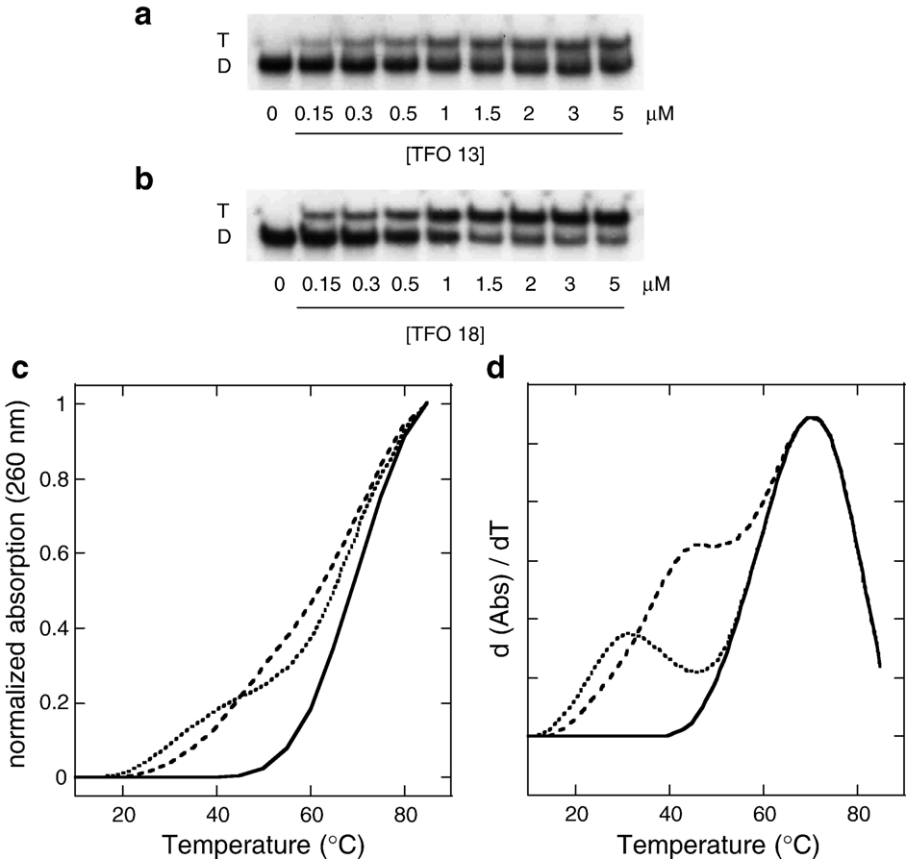

Fig. 3. Electrophoretic mobility shift assay (EMSA) of DNA mixtures containing DNA_{50} at fixed concentration (30 nM) and increasing concentrations (0.15, 0.3, 0.5, 1, 1.5, 2, 3 and 5 μM) of TFO_{13} (a) or TFO_{18} (b). D and T indicate duplex and triplex, respectively. (c) UV melting profiles of DNA_{30}+TFO_{13} (.....), DNA_{30}+TFO_{18} (- - - - -) and DNA_{30} (_____). (d) Derivatives of the thermal denaturation profiles shown in (c). The first two maxima correspond to the Tm of the triplex-to-duplex transitions and the last one to the Tm of DNA_{30}.

Jasco 715 spectropolarimeter equipped with a PTC 423S temperature controller.

Titrations of drug binding to triplex (DNA_{30}+TFO_{18} or DNA_{18}+TFO_{18}) and duplex (DNA_{30} or DNA_{18}) were carried out by dilution of initial samples containing 56 μM of each oligonucleotide component in 3 ml of 20 mM Tris–HCl pH 7.3, containing 50 mM NaCl, 5 mM $MgCl_2$ and 20 μM DAPER.

The initial DNAs/DAPER molar ratio (R) was fixed to 2.8, then it was decreased by dilution with a buffer solution containing 20 μM DAPER, so keeping constant the drug concentration throughout the titration.

The samples were equilibrated at 25 °C for 30 min prior to the scan. For each scan, two spectra were registered, distanced by 24 h, in a 1 cm path length cell at scanning rate of 200 and 2 nm/min, for UV and CD measurements. The scan of the buffer alone was subtracted from the average scan for each sample.

3. Results

3.1. Binding affinity of TFOs to the selected target sequence on hTERT promoter

Sequence analysis of the regulative region upstream of hTERT transcription initiation site (−1000/+1), led us to identify two homopurine–homopyrimidine sequences as possible targets for triple helix formation (Fig. 2a). The first sequence (−835/−814) partially overlaps to the putative binding site for Nuclear Factor 1 (NF1) [22] and is about one hundred nucleotides from the region involved in hormonal regulation [27]. The second sequence (−108/−90) is close to the transcription initiation site. The formation of DNA triple helical structure in one of these two regions could result in the inhibition of gene transcription.

In order to form DNA triplex structures, a target sequence must be accessible to TFOs. *In vivo* chromosomal DNA is packaged by histone proteins into nucleosomes [28], so that the accessibility of TFO target sequences will be significantly decreased in chromatin with respect to naked DNA [29–31].

To select the most accessible sequence to TFO between the target sequences identified on the hTERT promoter, we derived nucleosome positioning along the hTERT promoter region (−1000/+1) using the theoretical method, developed in our research group [24,25] and described in Section 2.3.

Using this method, a diagram of nucleosome positioning is obtained (Fig. 2b). The minima correspond to the minima of the free energy of nucleosome formation with respect to a standard random DNA sequence, marking the nucleosome dyad axis positions. While the first tract (−835/−814) is located within a region of comparatively stable nucleosomes, the tract close to the transcription initiation site (−108/−90) corresponds to a region that disfavors nucleosome formation.

This DNA tract is part of a major DNase I-hypersensitive site, experimentally evidenced in the hTERT promoter in telomerase positive cells by Wang and Zhu [23]; this finding suggests a relevant functional role of this DNA sequence in hTERT expression. Moreover, the selected sequence is located

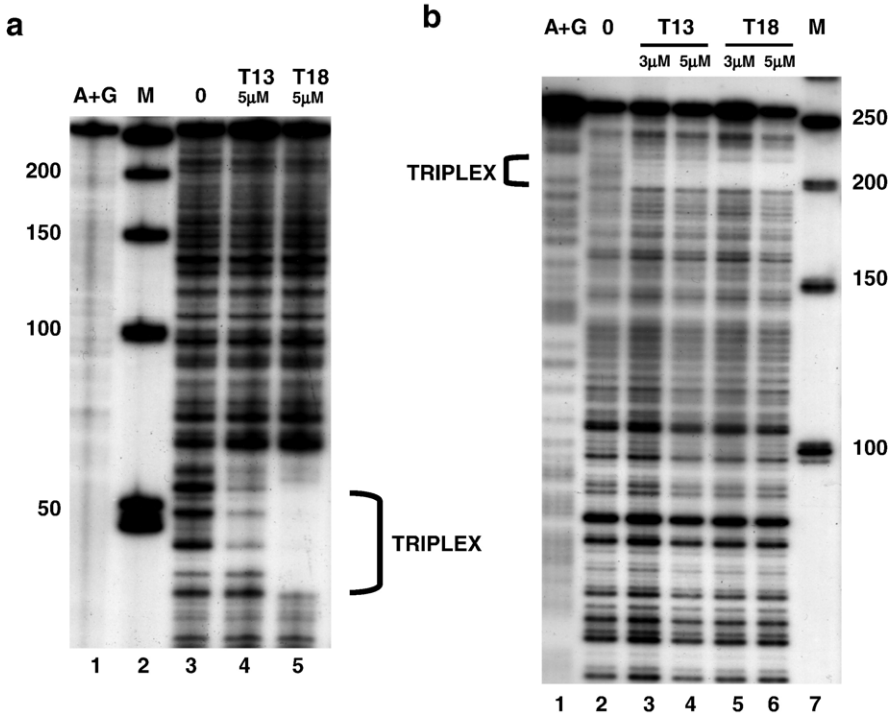

Fig. 4. (a) DNase I footprinting of the 260 bp hTERT promoter fragment (−309/−50) (hTERT F), radiolabeled at the 5′ end of G rich strand. Lane 1: Maxam and Gilbert reaction for purines. Lane 2: 50 bp ladder (M). Lane 3: DNase I cleavage of hTERT F. Lanes 4 and 5: DNase cleavage of hTERT F incubated with 5 μM of TFO_{13} (T_{13}) and TFO_{18} (T_{18}), respectively. (b) DNase I footprinting of hTERT F, radiolabeled at the 5′ end of C rich strand. Lane 1: Maxam and Gilbert reaction for purines. Lane 2: DNase I cleavage of hTERT F. Lanes 3–6: DNase cleavage of hTERT F incubated with 3 and 5 μM of TFO_{13} (T_{13}) (lanes 3 and 4) and of TFO_{18} (T_{18}) (lanes 5 and 6). Lane 7: 50 bp ladder (M).

within a region (−330/+360) that was shown to be essential for hTERT promoter activity [22].

Taking into account both theoretical and experimental data, we decided to focus our studies on the DNA tract from −108 to −90 bp.

Two homopurine TFOs were designed and synthesized to bind to the purine strand of DNA_{50} in anti-parallel orientation, overlapping the target sequence partially (TFO_{13}) or totally (TFO_{18}) (Fig. 1a and b).

To evaluate the affinity of TFO_{13} and TFO_{18} to the hTERT target, we carried out electrophoretic mobility shift assays (EMSA). To this end, a fixed amount (30 nM final concentration) of ^{32}P end labeled DNA_{50} (Fig. 1b) was incubated, with increasing concentrations of TFOs (0.15–5 μM), overnight at 37 °C to ensure equilibrium binding, as reported in previous studies [32,33]. Fig. 3 shows the electrophoretic patterns obtained for TFO_{13} (Fig. 3a) and for TFO_{18} (Fig. 3b) at 4 °C. Both TFO_{13} and TFO_{18} bind to DNA_{50}, decreasing their electrophoretic mobility, the latter more efficiently than the former.

To compare the binding of the two TFOs to duplex, the apparent association constants of triplex formation (K_a) were calculated as reported in Section 2.4 and correspond to K_a (TFO_{13}) ≈ 4.9×10^5 M^{-1} and K_a (TFO_{18}) ≈ 1.1×10^6 M^{-1}. These values satisfactorily agree to the melting temperatures of the triplexes formed by the two TFOs with DNA_{30}, as shown in Fig. 3c and d.

To confirm that the TFOs bind to duplex forming a triplex, a ^{32}P end-labeled fragment of the hTERT promoter 260 bp long (−309 to −50) (hTERT F, Fig. 2a), including the selected target sequence, was incubated with either TFO_{13} or TFO_{18} and subjected to DNase I digestion (Fig. 4). In these assays, the products of limited DNase I digestion were separated on a denaturing polyacrylamide gel (Fig. 4) and detected by autoradiography. The binding of both TFOs gives rise to a protected region corresponding to the target sequence in the hTERT promoter, as shown by autoradiographies. The protection is concentration dependent and is larger in the case of TFO_{18} than TFO_{13}. The densitometric analysis of the electrophoretic bands patterns (Supplementary Material) shows that the triplex is exactly localized on the target homopurine/homopyrimidine tract and does not cause any structural distortion of the duplex side sequences.

3.2. Stabilizing effect of the perylene derivative DAPER on triplex DNAs

To increase the stability of anti-parallel triplexes [12,34], we have studied the water soluble perylene derivative DAPER (Fig. 1c). Studying G-quadruplex stabilizing drugs [35,36], we have previously shown that DAPER is able to selectively bind to G-quadruplex structures with respect to duplex, on account of G-quadruplex larger aromatic area and higher charge density [37–39]. Both these features characterize also triplex structure with respect to duplex, suggesting us to investigate DAPER for its ability to bind and stabilize the anti-parallel triplexes [40].

EMSA has been carried out at constant concentration of TFO_{13} (3 μM) and DNA_{50} (30 nM) and at increasing amounts of DAPER (0.5–5 μM) (Fig. 5a). At 3 μM DAPER concentration the triplex formation is complete. In the case of TFO_{18}, similar results were obtained, except than the triplex formation is complete at 1 μM DAPER concentration (data not shown).

To obtain the triplex apparent association constants (K_a) in the presence of DAPER, we carried out EMSA at 4 °C, using TFO_{13} or TFO_{18} at increasing concentrations (5–50 nM) and DAPER fixed concentration (2 μM) (Fig. 5b). The values of K_a are about two orders of magnitude higher than in absence of DAPER (K_a (TFO_{13}) ≈ 6×10^7 M^{-1} and K_a (TFO_{18}) ≈ 7×10^7 M^{-1}).

DNase I footprinting studies of triplex, in the presence of DAPER, provided sound evidence that this ligand stabilizes triplex formation giving rise to a DNA clear protection from nuclease cleavage also at the lowest TFO concentration (0.5 μM) (Fig. 6). Also in the presence of DAPER, the autoradiography (Fig. 6) and the densitometric profiles (Supplementary material) show that the protection is precisely localized on the target sequence and that bordering duplex structure is not perturbed.

The antiparallel triplex formation requires the presence of Mg^{2+}, at least 5 mM [41], which mediates charges neutralization of the three anionic phosphodiester backbones. We carried out EMSA lowering $MgCl_2$ at physiological concentration (1 mM). In these experiments, constant concentrations of TFO_{13} (2 μM) and of DNA_{50} (30 nM) were used, increasing the concentration of DAPER from 0.5 to 3 μM. Fig. 5c shows that,

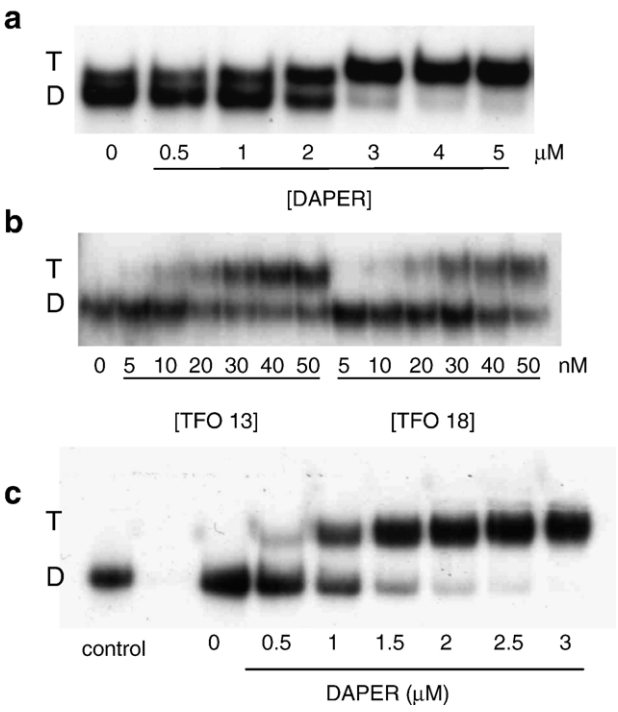

Fig. 5. (a) EMSA of DNA mixtures containing DNA_{50} at fixed concentration (30 nM) and TFO_{13} at concentration equal to 3 μM, in the presence of DAPER at increasing concentrations (0.5, 1, 2, 3, 4 and 5 μM). (b) EMSA of DNA mixtures containing DNA_{50} at fixed concentration (30 nM) and TFO_{13} (left) or TFO_{18} (right) at increasing concentrations (5, 10, 20, 30, 40 and 50 nM), in the presence of 2 μM DAPER. D and T indicate duplex and triplex, respectively. (c) EMSA of DNA mixtures containing DNA_{50} (30 nM), TFO_{18} (2 μM) and increasing concentrations of DAPER (0.5, 1, 1.5, 2, 2.5, and 3 μM). $MgCl_2$ concentration was fixed at 1 mM. The electrophoretic shift of DNA_{50} was used as control.

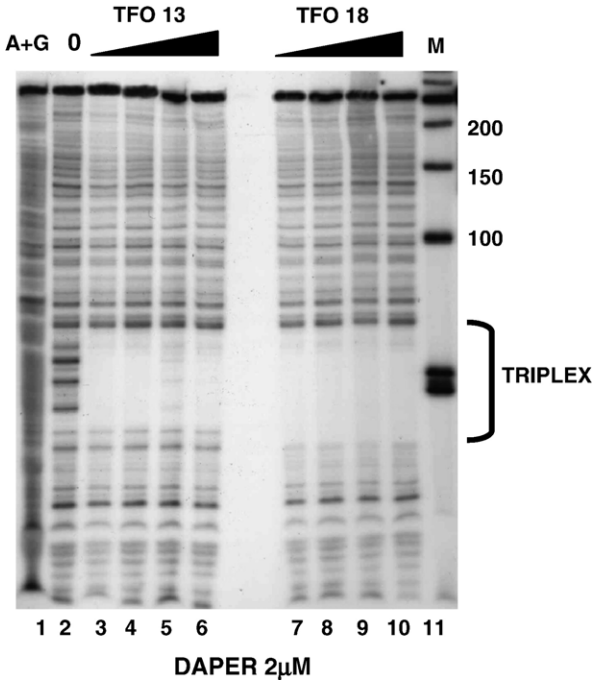

Fig. 6. (a) DNase I footprinting of hTERT F, radiolabeled at the 5′ end of G rich strand, in the presence of DAPER 2 μM and TFO_{13} (lanes 3–6) or TFO_{18} (lanes 7–10) at increasing concentrations (0.5, 1, 2 and 4 μM). Lane 1: Maxam and Gilbert reaction for purines. Lane 2: DNase I cleavage of hTERT F. Lane 11: 50 bp ladder (M).

at lower Mg^{2+} concentration, the presence of DAPER becomes critical for the triplex formation. In fact, without the ligand, the triplex is not detectable, while in the presence of increasing DAPER concentration, increasing triplex amounts were obtained. At 3 μM DAPER concentration only the triplex was present.

Furthermore, we have analyzed the triplex/DAPER complex stability, replacing Na^+ with K^+ [42]. The results, reported in Supplementary Material, show that, increasing the drug concentration from 2 μM up to 10 μM, the triplex concentration increases, becoming almost the prevalent structure at the highest DAPER concentration. In this case, an higher concentration of DAPER, than in the presence of Na^+, is needed for triplex formation.

Increasing $MgCl_2$ concentration to 5 mM, the DAPER concentration needed to stabilize the triplex is lower (Supplementary material), showing that DAPER and Mg^+ act jointly in stabilizing triplex.

3.3. Absorption and circular dichroism spectroscopy of DAPER binding to triplex and duplex DNAs

In order to characterize the molecular features of DAPER binding to triplex in comparison with duplex DNA, we carried out absorption spectroscopy and circular dichroism studies of drug electronic transitions in the wavelength range from 400 to 650 nm, in the presence of either duplex (DNA_{30} and DNA_{18}) or triplex ($DNA_{30}+TFO_{18}$ and $DNA_{18}+TFO_{18}$).

Absorption spectra of the complexes of DAPER with either triplex or duplex DNAs, at different DNAs/drug molar ratios (R) and constant drug concentration, were carried out. The spectrum of DAPER in water solution is characterized by a broad band centered at ≈497 nm, with a shoulder at 530 nm [26]. In presence of the two DNA structures, the absorption profile of DAPER changes (Fig. 7a and b): increasing R, it becomes similar to that obtained in organic solvents [26], characterized by three maxima at 525, 475 and 450 nm, except than the three bands are red-shifted of about 25 nm each. The variation of the absorption spectra of triplex/DAPER and duplex/DAPER complexes as function of R is very similar (Fig. 7c). This indicates that both DNA structures induce DAPER unstacking.

Taking into account the complexity of possible equilibria between DAPER free and bound to DNAs, in stacked or unstacked form, Circular Dichroism (CD) spectroscopy appears more suitable than absorption spectroscopy [43] to study the

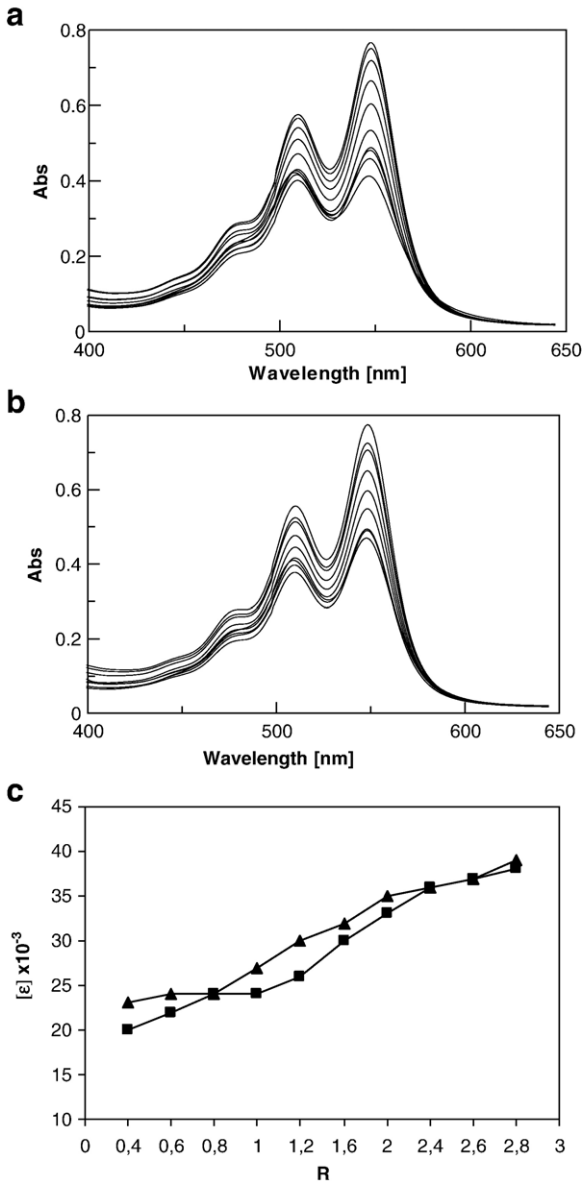

Fig. 7. Absorption spectra of DAPER at increasing concentration of DNA triplex (a) and duplex (b). (c) Extinction coefficients at 550 nm as function of R (DNAs/drug molar ratio), in the case of duplex (▲) and triplex (■).

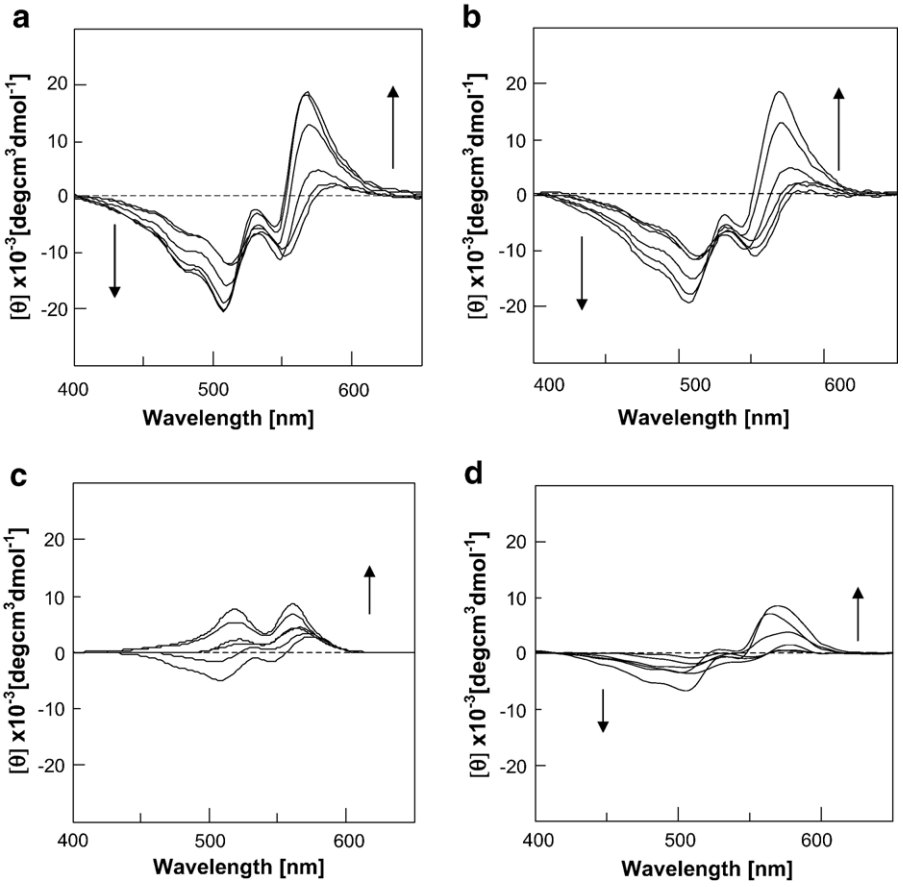

Fig. 8. CD titrations of triplex–DAPER complexes (DNA_{30}+TFO_{18})/DAPER in (a), (DNA_{18}+TFO_{18})/DAPER in (b) and duplex–DAPER complexes (DNA_{30})/DAPER in (c), (DNA_{18}) /DAPER in (d). The CD spectra are reported for *R* (DNAs/drug molar ratio) from 2.4 to 0.4 with decreasing steps of 0.4. The arrows point out the increasing in the amplitude of CD band with decreasing *R* values.

drug binding. In fact, since DAPER is a symmetric molecule, it is not optically active. DNA shows a CD spectrum only in the wavelength range from 220 to 320 nm, so that CD spectra of complexes between DNAs and DAPER, in the wavelength range from 400 to 650 nm, are exclusively due to the ligand molecules bound to DNA and asymmetrically perturbed.

CD analysis were carried out, recording the spectra of solutions of two triplex (DNA_{30}+TFO_{18} and DNA_{18}+TFO_{18}) and two duplex (DNA_{30} and DNA_{18}) with DAPER at decreasing DNAs/drug molar ratios (*R*), from 2.8 to 0.4, while the DAPER concentration (20 μM) was kept constant (Fig. 8).

In Fig. 8a the CD spectra of triplex (DNA_{30}+TFO_{18})/DAPER complexes at different *R* are reported. At *R* higher than 1.2, the spectra are characterized by two minima at 512 and 552 nm and a modest positive band centered at about 565 nm. Surprisingly, decreasing the *R* value and, thus, the number of triplex binding sites, the ellipticity values of the maximum at 565 nm and those of the two minima strongly increase.

The variations of CD spectra as function of *R*, in the case of triplex (DNA_{18}+TFO_{18})/DAPER, reported in Fig. 8b are equal to those obtained with triplex (DNA_{30}+TFO_{18}), reported in Fig. 8a.

At higher *R* values, the ellipticity characterizing the spectra of duplex (DNA_{30})/DAPER complexes, is similar to that of triplex, although it is significantly lower. At lower *R* values (lower DNA concentrations), the duplex/DAPER CD spectra show different features than the corresponding spectra referring to triplex (Fig. 8c), being characterized by two large positive bands, at about 525 and 560 nm.

The complexes duplex (DNA_{18}) /DAPER show CD spectra with the same features than triplex, both at high and low *R* (Fig. 8d); also in this case, the ellipticities are significantly reduced, with respect to triplex–DAPER complexes.

4. Discussion

This study shows that the homopurine–homopyrimidine tract, selected on hTERT promoter (−108/−90), should be a good target for the antigene strategy, based on triple helix formation.

The selection between different homopurine–homopyrimidine DNA tracts on hTERT promoter was based on their chromatin organization and is supported by a number of researches both *in vitro* and *in vivo*, suggesting a decreased target accessibility to TFOs in the nucleosomal environment [29–31].

Recently, Wang and Zhu [23] found a major DNase I hypersensitive site (corresponding to chromatin accessible region, characterized by less stable nucleosomes) within 100 bp upstream of the transcription start site of hTERT gene, in several hTERT expressing immortal cell lines. The same region is not characterized by DNase I hypersensitive sites in

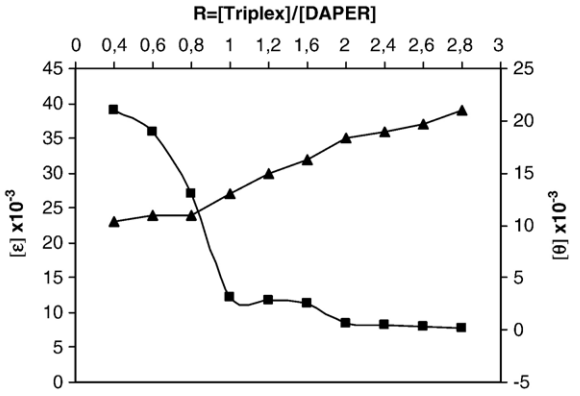

Fig. 9. Extinction coefficients at 550 nm ([ε]) (▲) and ellipticity ([θ]) (■) at 575 nm as function of *R*, in the case of triplex (DNA_{30}+TFO_{18})/DAPER complexes.

cells, where hTERT is not expressed. These experimental data support the theoretical analysis of sequence dependent nucleosome positioning on hTERT promoter, that evidenced a "quasi hole" in the nucleosomes organization, close to the transcription initiation site, centered at the homopurine–homopyrimidine tract (−108/−90) (Fig. 2b). Indeed, both experimental and theoretical studies suggest a relevant functional role of the homopurine–homopyrimidine tract (−108/−90) in hTERT expression. It is worth noting that, in this case, the correlation between theoretical and experimental data is quite satisfactory; however, experimental and theoretical studies of a number of different biological systems are necessary to generalize the theoretical approach to select favorable TFOs target in a chromatin context.

Using appropriate TFOs, we have shown that the hTERT promoter tract (−108/−90) forms anti-parallel triplex, characterized by satisfactory stability both by EMSA and UV absorption melting temperatures analysis. Furthermore, the interactions between the target and the TFOs appear well localized without perturbation of adjacent duplex structure, at least in the promoter region from −309 to −50, as shown by DNase I footprinting analysis.

An important task to pursue in controlling gene expression by triple helix strategy, is the stability of this structure in physiological conditions [44]. Several modifications of the sugar-phosphate backbone as well as of nucleotides have been developed to improve triple helix stability and specificity [45]. Another way to increase the stability of triplex consists in using ligands which bind selectively to triplex, shifting the equilibrium between duplex and triplex towards the latter [12].

Using EMSA and DNase I footprinting, we have found that the triplex stability is significantly increased in the presence of the water soluble perylene derivative, DAPER. Moreover, in the presence of DAPER, the concentration of the TFOs necessary to form an anti-parallel triplex can be significantly reduced, also at Mg^{2+} physiological concentration (Fig. 5c). If K^+ replaces Na^+, the drug is able to stabilize triplex, although at higher concentration than in the presence of Na^+ (Supplementary Material).

As previously reported in the case of perylene molecules with hydrophobic side chains, studied in organic solvents, the stacking of disk-shaped molecules generates one-dimensional aggregates in solution and the aggregation can be ascribed to strong π−π interactions among such discotic molecules [46].

In the case of perylene derivatives with positively charged side chains (such as DAPER), electrostatic interactions with DNA should produce asymmetrically perturbed electronic transitions and the strong coupling between nearest-neighbor perylene molecules give rise to CD spectra characterized by splitted positive and negative bands for the S_0–S_1 transition of perylene chromophore at 517 nm. Also the vibronic structure, that can be ascribed to the vibration of perylene skeleton, which is strongly coupled with the S_0–S_1 transition, should be characterized by the same splitting, at about 550 and 475 nm [47].

We suggest that the complex CD spectra, in Fig. 8, could derive from the combination of Cotton effects associated with the three transitions, whose crossovers are about 550, 525 and 475 nm, as a result of the binding of self-stacked DAPER molecules around triple or duplex DNA, following their helical structure.

The increase of DNA concentration produces a progressive unstacking of the free DAPER molecules in solution as well as along the narrow grooves. In fact as shown in Fig. 9, the unstacking, as measured by the increase of extinction coefficient at 550 nm, corresponds to the decrease of ellipticity at 575 nm (Fig. 9).

The general pattern of absorption and CD spectra of the electronic transitions of DAPER shown in Figs. 7 and 8 suggests a possible model of the association complexes with duplex and triplex DNA.

The absorption spectra show a regular increasing of the extinction coefficient with increasing triplex or duplex DNA concentration monitoring the progressive unstaking of the drug

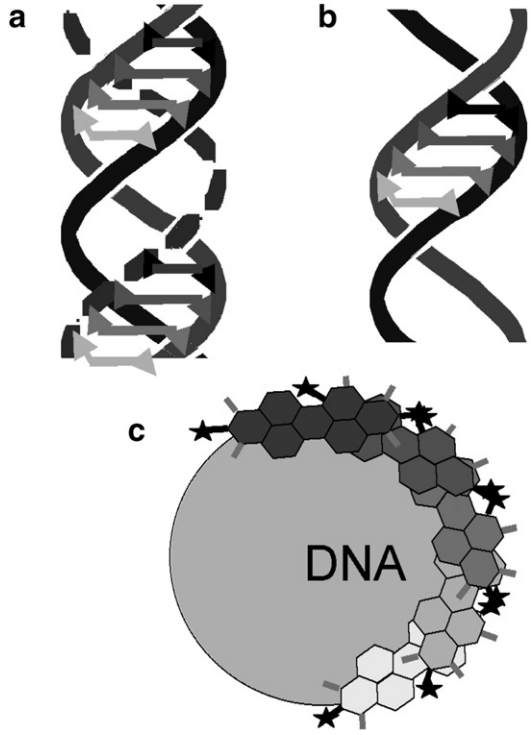

Fig. 10. Pictorial drawing along (a–b) and perpendicular (c) to the DNA helical axis of the molecular model of triplex–DAPER (a) and duplex–DAPER (b) complexes, at low DNA concentration, where the DAPER molecules are self-stacked. The stars represent the DAPER cationic side chains (c).

molecules (Fig. 7). Such a trend is at odd with that of the CD spectra, which show ellipticity decreasing in spite of the increasing concentration of DNA, the asymmetric partner of the association complexes. Thus the highest ellipticity is obtained at the lowest DNA/DAPER ratio available (Fig. 9), which can be reached, without significant aggregation.

We propose that the observed Cotton effects are due to the asymmetric, helical, stacking of the DAPER molecules induced by the regular electrostatic interactions of the cationic side chains with the phosphate anionic sequence along the narrow grooves of the duplex and triplex, according to the proposed model reported in Fig. 10. In the latter case such sterospecific interactions occur three times more than in the double helix, since, in the case of duplex, only one narrow groove is present, instead of the three narrow grooves characterizing the triplex.

The main features of the proposed model (Fig. 10) are the result of the coherent electrostatic interactions of the DAPER cationic side chains with the sequence of the phosphate groups of pairs of DNA strands favored by the drug self -stacking. The model explains the ability of DAPER to increase the thermodynamic stability of the triplex structure.

Such model offers an interpretation also for the different CD spectra of duplex DNA_{30} with respect to DNA_{18}, at low *R*. In fact, at lower DNA concentration DAPER could bind also to major grooves with a different contribution to the CD spectra. This is not possible in the case of DNA_{18}, which is too short to form an effective large groove. Such consideration explains also the practical identity of CD spectra of triplex complexes that TFO_{18} forms with the DNA_{30} and DNA_{18}. In fact, in the case of the triplex ($DNA_{30}+TFO_{18}$) complexes, the two duplex terminal tracts are too short to form the large groove; therefore only narrow grooves are present in both structures.

5. Conclusions

The results, obtained in this study, indicate that the sequence selected on hTERT promoter can be a useful target for triple helix formation. Furthermore, the investigated anti-parallel triplex on this DNA tract is effectively stabilized by DAPER, suggesting the opportunity to synthesize DAPER-TFO conjugates. The drug binding appears to be significantly larger to triplex with respect to duplex in agreement with the proposed model, characterized by DAPER self-stacking along triplex or duplex narrow grooves. The model satisfactorily accounts for the larger than twice increase in molar ellipticity in triplex–DAPER complex with respect to that with duplex.

In conclusion, a new method to inhibit telomerase, based on antigen strategy, seems possible. On account of DAPER–hydrophobic perylene moiety, DAPER–TFO conjugates could be useful also to solve the problems of TFOs internalization. This is currently under investigation in our research group.

Acknowledgements

The plasmid p1009 was a kind gift of S. Bacchetti. This work was supported by PRIN 2005 and by Istituto Pasteur-Fondazione Cenci Bolognetti.

Appendix A. Supplementary data

Supplementary data associated with this article can be found, in the online version, at doi:10.1016/j.bpc.2007.05.009.

References

[1] D. Rhodes, L. Fairall, T. Simonsson, R. Court, L. Chapman, Telomere architecture, EMBO Rep. 3 (2002) 1139–1145.
[2] E.H. Blackburn, Telomeres and telomerase: their mechanisms of action and the effects of altering their functions, FEBS Lett. 579 (2005) 859–862.
[3] M. O'Reilly, S.A. Teichmann, D. Rhodes, Telomerases, Curr. Opin. Struct. Biol. 9 (1999) 56–65.
[4] J.W. Shay, W.E. Wright, Senescence and immortalization: role of telomeres and telomerase, Carcinogenesis 26 (2005) 867–874.
[5] E. Pascolo, C. Wenz, J. Lingner, N. Hauel, H. Priepke, I. Kauffmann, P. Garin-Chesa, W.J. Rettig, K. Damm, A. Schnapp, Mechanism of human telomerase inhibition by BIBR1532, a synthetic, non-nucleosidic drug candidate, J. Biol. Chem. 277 (2002) 15566–15572.
[6] J.L. Mergny, J.F. Riou, P. Maillieet, M.P. Teulade-Richou, E. Gilson, Natural and pharmacological regulation of telomerase, Nucleic Acids Res. 30 (2002) 839–865.
[7] L.R. Kelland, Overcoming the immortality of tumour cells by telomere and telomerase based cancer therapeutics — current status and future prospects, Eur. J. Cancer 41 (2005) 971–979.
[8] J.B. Opalinska, A.M. Gewirtz, Nucleic-acid therapeutics: basic principles and recent applications, Nat. Rev. Drug Discovery 1 (2002) 503–514.
[9] U. Galderisi, A. Cascino, A. Giordano, Antisense oligonucleotides as therapeutic agents, J. Cell. Physiol. 181 (1999) 251–257.
[10] M.M. Seidman, P.M. Glazer, The potential for gene repair via triple helix formation, J. Clin. Invest. 112 (2003) 487–494.
[11] J. Volker, H.H. Klump, Electrostatic effects in DNA triple helices, Biochemistry 33 (1994) 13502–13508.
[12] R. Besch, C. Giovannangeli, K. Degitz, Triplex-forming oligonucleotides — sequence-specific DNA ligands as tools for gene inhibition and for modulation of DNA-associated functions, Curr. Drug Targets 5 (2004) 691–703.
[13] M. Alunni-Fabbroni, D. Pirulli, G. Manzini, L.E. Xodo, (A,G)-oligonucleotides form extraordinary stable triple helices with a critical R.Y sequence of the murine c-Ki-ras promoter and inhibit transcription in transfected NIH 3T3 cells, Biochemistry 35 (1996) 16361–16369.
[14] L.E. Xodo, T. Rathinavelan, F. Quadrifoglio, G. Manzini, N. Yathindra, Targeting neighbouring poly(purine-pyrimidine) sequences located in the human bcr promoter by triplex-forming oligonucleotides, Eur. J. Biochem. 268 (2001) 656–664.
[15] F. Svinarchuk, A. Debin, J.R. Bertrand, C. Malvy, Investigation of the intracellular stability and formation of a triple helix formed with a short purine oligonucleotides targeted to the murine c-pim-1 proto-oncogene promoter, Nucleic Acids Res. 24 (1996) 295–302.
[16] G.M. Carbone, E.M. McGuffie, A. Collier, C.V. Catapano, Selective inhibition of transcription of the Ets2 gene in prostate cancer cells by a triplex-forming oligonucleotide, Nucleic Acids Res. 31 (2003) 833–843.
[17] V. Rapozzi, S. Cogoi, P. Spessotto, A. Risso, G.M. Bonora, F. Quadrifoglio, L.E. Xodo, Antigene effect in K562 cells of a PEG-conjugated triplex-forming oligonucleotide targeted to the bcr/abl oncogene, Biochemistry 41 (2002) 502–510.
[18] K.J. Wu, C. Grandori, M. Amacker, N. Simon-Vermot, A. Polack, J. Lingner, R. Dalla-Favera, Direct activation of TERT transcription by c-MYC, Nat. Genet. 21 (1999) 220–224.
[19] S. Kyo, M. Takakura, T. Taira, T. Kanaya, H. Itoh, M. Yutsudo, H. Ariga, M. Inoue, Sp1 cooperates with c-Myc to activate transcription of the human telomerase reverse transcriptase gene (hTERT), Nucleic Acids Res. 28 (2000) 669–677.
[20] X. Xiao, M. Athanasiou, I.A. Sidorov, I. Horikawa, G. Cremona, D. Blair, J.C. Barret, D.S. Dimitrov, Role of Ets/Id proteins for telomerase regulation in human cancer cells, Exp. Mol. Pathol. 75 (2003) 238–247.
[21] S. Nanni, M. Narducci, L. Della Pietra, F. Moretti, A. Grasselli, P. De Carli, A. Sacchi, A. Pontecorvi, A. Farsetti, Signaling through estrogen receptors

modulates telomerase activity in human prostate cancer, J. Clin. Invest. 110 (2002) 219–227.
[22] Y.S. Cong, J. Wen, S. Bacchetti, The human telomerase catalytic subunit hTERT: organization of the gene and characterization of the promoter, Hum. Mol. Genet. 8 (1999) 137–142.
[23] S. Wang, J. Zhu, The hTERT gene is embedded in a nuclease-resistant chromatin domain, J. Biol. Chem. 279 (2004) 55401–55410.
[24] C. Anselmi, G. Bocchinfuso, P. De Santis, M. Savino, A. Scipioni, Dual role of DNA intrinsic curvature and flexibility in determining nucleosome stability, J. Mol. Biol. 286 (1999) 1293–1301.
[25] C. Anselmi, P. De Santis, R. Paparcone, M. Savino, A. Scipioni, From the sequence to the superstructural properties of DNAs, Biophys. Chemist. 95 (2002) 23–47.
[26] Z.R. Liu, R.L. Rill, *N,N′*-Bis[3,3′-(dimethylamino)propylamine]-3,4,9,10 perylenetetracarboxylic diimide, a dicationic perylene dye for rapid precipitation and quantization of trace amounts of DNA, Anal. Biochem. 236 (1996) 139–145.
[27] S. Misiti, S. Nanni, G. Fontemaggi, Y.S. Cong, J. Wen, H.W. Hirte, G. Piaggio, A. Sacchi, A. Pontecorvi, S. Bacchetti, A. Farsetti, Induction of hTERT expression and telomerase activity by estrogens in human ovary epithelium cells, Mol. Cell. Biol. 20 (2000) 3764–3771.
[28] K. Luger, A.W. Mader, R.K. Richmond, D.F. Sargent, T.J. Richmond, Crystal structure of the nucleosome core particle at 2.8 A resolution, Nature 389 (1997) 251–260.
[29] P.M. Brown, K.R. Fox, Nucleosome core particles inhibit DNA triple helix formation, Biochem. J. 319 (1996) 607–611.
[30] M.L. Espinas, E. Jimenez-Garcia, A. Martinez-Balbas, F. Azorin, Formation of triple-stranded DNA at d(GAxTC)n sequences prevents nucleosome assembly and is hindered by nucleosomes, J. Biol. Chem. 271 (1996) 31807–31812.
[31] R. Besch, C. Giovannangeli, T. Schuh, C. Kammerbauer, K. Degitz, Characterization and quantification of triple helix formation in chromosomal DNA, J. Mol. Biol. 341 (2004) 979–989.
[32] J.G. Hacia, B.J. Wold, P.B. Dervan, Phosphorothioate oligonucleotide-directed triple helix formation, Biochemistry 33 (1994) 5367–5369.
[33] E.M. McGuffie, D. Pacheco, G.M. Carbone, C.V. Catapano, Antigene and antiproliferative effects of a c-*myc*-targeting phosphorothioate triple helix-forming oligonucleotide in human leukemia cells, Cancer Res. 60 (2000) 3790–3799.
[34] M.D. Keppler, P.L. James, S. Neidle, T. Brown, K.R. Fox, DNA sequence specificity of triplex-binding ligands, Eur. J. Biochem. 270 (2003) 4982–4992.
[35] E.M. Rezler, D.J. Bears, L.H. Hurley, DNA tetraplex-binding drugs: structure-selective targeting is critical for antitumour telomerase inhibition, Mini Rev. Med. Chem. 1 (2001) 31–41.
[36] J. Casals, L. Debethune, K. Alvarez, A. Risitano, K.R. Fox, A. Grandas, E. Pedroso, Directing quadruplex stabilizing drugs into the telomere: synthesis and properties of acridine-oligonucleotide conjugates, Bioconjug. Chem. 17 (2006) 1351–1359.
[37] O.Y. Fedoroff, M. Salazar, H. Han, V.V. Chemeris, S.M. Kerwin, L.H. Hurley, NMR-based model of a telomerase-inhibiting compound bound to G-quadruplex DNA, Biochemistry 37 (1998) 12367–12374.
[38] L. Rossetti, M. Franceschin, A. Bianco, G. Ortaggi, M. Savino, Perylene diimides with different side chains are selective in inducing different G-quadruplex DNA structures and in inhibiting telomerase, Bioorg. Med. Chem. Lett. 12 (2002) 2527–2533.
[39] L. Rossetti, M. Franceschin, S. Schirripa, A. Bianco, G. Ortaggi, M. Savino, Selective interactions of perylene derivatives having different side chains with inter- and intra-molecular G-quadruplex DNA structures. A correlation with telomerase inhibition, Bioorg. Med. Chem. Lett. 15 (2005) 413–420.
[40] S. Bevers, S. Shutte, L.W. McLaughlin, Naphthalene- and perylene-based linkers for the stabilization of hairpin triplex, J. Am. Chem. Soc. 122 (2000) 5905–5915.
[41] S.W. Blume, J. Lebowitz, W. Zacharias, V. Guarcello, C.A. Mayfield, S.W. Ebbinghaus, P. Bates, D.E. Jones, J. Trent, N. Vigneswaran, D.M. Miller, The integral divalent cation within the intermolecular purine*purine. pyrimidine structure: a variable determinant of the potential for and characteristics of the triple helical association, Nucleic Acids Res. 27 (1999) 695–702.
[42] Y. Cheng, N. Korolev, L. Nordenskiold, Similarities and differences in interaction of Na^+ and K^+ with condensed ordered DNA. A molecular dynamics computer simulation study, Nucleic Acids Res. 34 (2006) 686–696.
[43] T.C. Jenkins, Optical absorbance and fluorescence techniques for measuring DNA–drug interactions, Methods Mol. Biol. 90 (1997) 195–218.
[44] R.W. Roberts, D.M. Crothers, Prediction of the stability of DNA triplexes, Proc. Natl. Acad. Sci. 93 (1996) 4320–4325.
[45] K.R. Fox, Targeting DNA with triplexes, Curr. Med. Chem. 7 (2000) 17–37.
[46] Z. Chen, V. Stepanenko, V. Dehm, P. Prins, L.D. Siebbeles, J. Seibt, P. Marquetand, V. Engel, F. Wurthner, Photoluminescence and conductivity of self-assembled π–π stacks of perylene bisimide dyes, Chemistry 13 (2007) 436–449.
[47] M. Sadrai, L. Hadel, R.R. Sauers, S. Husain, K. Krogh-Jespersen, J.D. Westbrook, G.R. Bird, Lasing action in a family of perylene derivatives: singlet absorption and emission spectra, triplet absorption and oxygen quenching constants and molecular mechanics and semiempirical molecular orbital calculations, J. Phys. Chem. 96 (1992) 7988–7996.